ELSEVIER

Biochimica et Biophysica Acta 1553 (2002) 212–217

BIOCHIMICA ET BIOPHYSICA ACTA
BBA

www.bba-direct.com

Density functional calculations modelling tyrosine oxidation in oxygenic photosynthetic electron transfer

Patrick J. O'Malley *

Department of Chemistry, UMIST, Manchester M60 1QD, UK

Received 3 July 2001; received in revised form 25 September 2001; accepted 26 September 2001

Abstract

Hybrid density functional calculations are used to model tyrosine oxidation during electron transfer reactions of photosystem II. The predicted frequency values for the 7a and δCOH modes of the reduced form and the 7a mode of the oxidised radical form are in excellent agreement with experimental data obtained for Mn and Ca depleted systems by Hienerwadel et al. [Biochemistry 36 (1997) 15447] and Berthomieu et al. [Biochemistry 37 (1998) 10547]. The calculations confirm that the two tyrosines Y_D and Y_Z are protonated in the reduced form. On oxidation the larger 7a frequency value observed experimentally for Y_Z• can be best explained by a greater localisation of the protonic charge released on formation of this tyrosyl free radical.

1. Introduction

Tyrosine (Y) has been shown to be a key electron transfer agent in a wide number of biological systems [1–6]. Of particular importance is the role played by the tyrosine/tyrosyl redox couple in the electron and proton transfer reactions leading to the oxidation of water to molecular oxygen in the photosystem II (PSII) reaction centre of green plant photosynthesis.

Two tyrosine amino acid residues, D2-Tyr160 (Y_D) and D1-Tyr161 (Y_Z), are oxidised by the electron transfer reactions of PSII [1]. Y_D is apparently bypassed in the electron transfer reactions between the site of water oxidation (a manganese cluster) and the primary oxidant chlorophyll (P680). It appears as a relatively stable neutral tyrosyl radical. Y_Z on the other hand serves as an electron transfer intermediate between the manganese cluster and P680. An additional function, serving as a hydrogen abstractor from the water molecules attached to the manganese cluster, has recently been ascribed to this tyrosine residue [7]. In the reduced state the phenolic OH groups of both tyrosine residues have been proposed to act as hydrogen bond donors to one of the imidazole nitrogens of a nearby histidine residue, i.e. D2-His189 for Y_D and D1-His190 for Y_Z (*Synechocystis* numbering). Upon oxidation it is suggested that the hydroxyl hydrogen transfers to the imidazole nitrogen of the histidine (see [7,8] for details. Some studies have however suggested that both tyrosines are deprotonated in the reduced state existing as tyrosinate residues [9,10].

Fourier transform infrared (FTIR) difference spectroscopy is a valuable tool in monitoring the changes occurring in the cofactors involved in electron transfer [11]. Direct information on both the ground state and the oxidised or reduced forms of the electron transfer intermediates can be obtained. For the tyro-

* Tel.: +44-161-236-3311; Fax: +44-161-228-7040.
E-mail address: p.o'malley@umist.ac.uk (P.J. O'Malley).

0005-2728/01/$ – see front matter
PII: S0005-2728(01)00222-5

sine residues involved in PSII the technique has been used to monitor the oxidation of both tyrosine residues mentioned above [12,13]. The presence of a band assigned to the COH bending mode for both tyrosines in the reduced state appeared to provide direct evidence that both are protonated prior to oxidation [12,13]. There is however disagreement on the correct band assignment and interpretation of the FTIR difference spectra of both Y_D and Y_Z. In a recent paper Barry and coworkers [14] have argued against previous assignments [12,13] suggesting that the spectra were compromised by "the deleterious buffer conditions employed". To help clarify this situation we report here on density functional calculations (B3LYP) performed on model tyrosine hydrogen bonded complexes, in the reduced and oxidised state. These allow us to accurately predict the relevant vibrational frequencies and modes of the model complexes used. In such a fashion we clarify the experimental assignments as well as providing a deeper insight into the factors governing the vibrational characteristics of tyrosine and tyrosyl free radicals.

Previous studies [15–17] have also used density functional calculations to study phenoxyl free radicals and predict vibrational frequencies. These previous studies have concentrated on the isolated radical and have not studied the effect of hydrogen bonding between the phenoxyl oxygen and proton donors.

2. Materials and methods

The density functional calculations were performed using the B3LYP functional combined with the EPR-II basis set. The details of the calculation procedure have been described previously [18]. The tyrosine model complexes are shown in Figs. 1 and 2. The principal models used, Fig. 1, were *p*-cresol (MePH), *p*-cresol/imidazole (MePH-IM), *p*-cresyl/imidazolium ion (MeP-IMH$^+$•) and *p*-cresyl/imidazole (MeP-IM•). In addition further hydrogen bonded models MePH-IM-HB (Fig. 2a), MeP-IMH-HB$^+$• (Fig. 2b) and MeP-IM-HB• (Fig. 2c) were studied to investigate the effect of further hydrogen bonding to the imidazole or imidazolium group. Experimental studies on tyrosine and *p*-cresol [12] indicate that the 7a and δCOH bending vibrations are essentially identical for both suggesting that further extension of the models beyond *p*-cresol can be expected to have little influence on the calculated values. The calculated harmonic frequencies were scaled by 0.980 (7a) and 0.983 (δCOH) to allow comparison with experimental anharmonic values. These

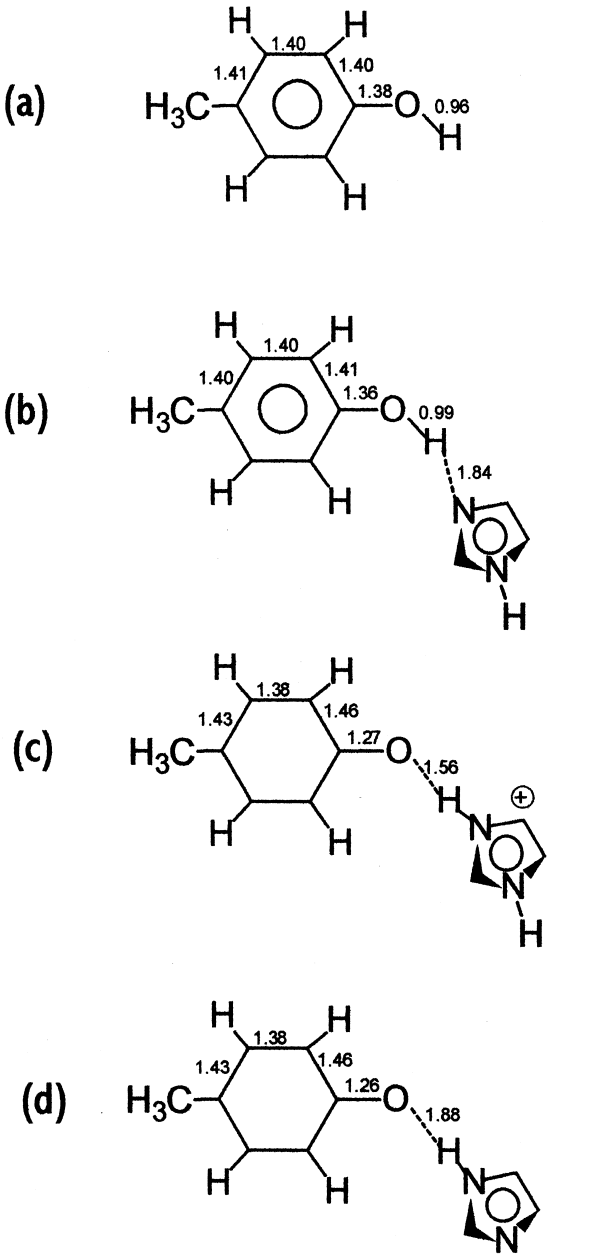

Fig. 1. Model complexes used for the calculations: (a) MePH, (b) MePH-IM, (c) MeP-IMH$^+$• and (d) MeP-IM•. Selected optimised bond distances are given in Å. The optimised angle between the imidazole/imidazolium and phenol/phenoxyl ring planes is 90° for b, 59° for c and 74° for d.

scaling factors were derived by comparing experimentally determined 7a and δCOH vibration frequencies for gas phase phenol with calculations performed at the level reported here.

3. Results and discussion

The optimised bond distances for each model studied are given in Figs. 1 and 2. Upon oxidation of MePH-IM and MePH-IM-HB proton transfer occurs simultaneously, without an energy barrier, from the phenol to the imidazole which then back hydrogen bonds with the oxygen atom of the phenoxyl radical in MeP-IMH^{+}• and MeP-IMH-HB^{+}•. The scaled harmonic frequencies calculated for MePH, MePH-IM and MePH-IM-HB, for the 7a CO stretching and the δCOH bending vibrational modes, are presented in Table 1 where they are compared with experimental values for *p*-cresol and a *p*-cresol–imidazole complex [12]. The data for the extended model Me-PH-IM-HB are essentially identical to the smaller Me-PH-IM model indicating that additional hydrogen bonding to the imidazole produces little change to the calculated stretching and bending frequencies. The trends in frequency changes observed experimentally are well reproduced by the calculations. In essence the increased frequency value of both modes on hydrogen bond formation of the phenol OH group with imidazole is quantitatively reproduced. In addition the relatively increased intensity of the δCOH bending mode relative to the CO stretch mode, on hydrogen bond formation, is also well reproduced. The frequency values for the two redox active tyrosines of PSII, Y_D and Y_Z (Table 1), are also close to the MePH-IM and MePH-IM-HB models providing supporting evidence that both correspond to protonated tyrosine residues hydrogen bonded to an imidazole group of a nearby histidine residue. In Table 1 the shifts in frequency observed on isotopic substitution are also presented. Downshifts in both modes are predicted for $^{13}C(4)$ and $^{13}C_6$ isotopomers. For the $^{2}H_4$ form only one intense mode (principally CO stretching) is predicted to appear. The predicted frequency values are in excellent agreement with those reported for both Y_D and Y_Z. The experimentally detected bands can be clearly ascribed to the downshifted δCOH mode for the $^{13}C(4)$ and $^{13}C_6$ isotopomers. Due to the differential nature of the FTIR experiment the downshifted 7a mode cannot be detected experimentally [12,13]. For the $^{2}H_4$ isotopomer the calculations suggest that the single band detected experimentally [12] is due to the downshifted CO stretching mode. These calculations provide confirmation of the assignments given in [12,13] and indicate that both Y_Z and Y_D are *protonated* tyrosines which are hydrogen bonded to nearby imidazole groups of neighbouring histidine residues. One electron oxidation of MePH-IM and MePH-IM-HB leads to simultaneous transfer of the phenol proton to the hydrogen bonded imidazole as

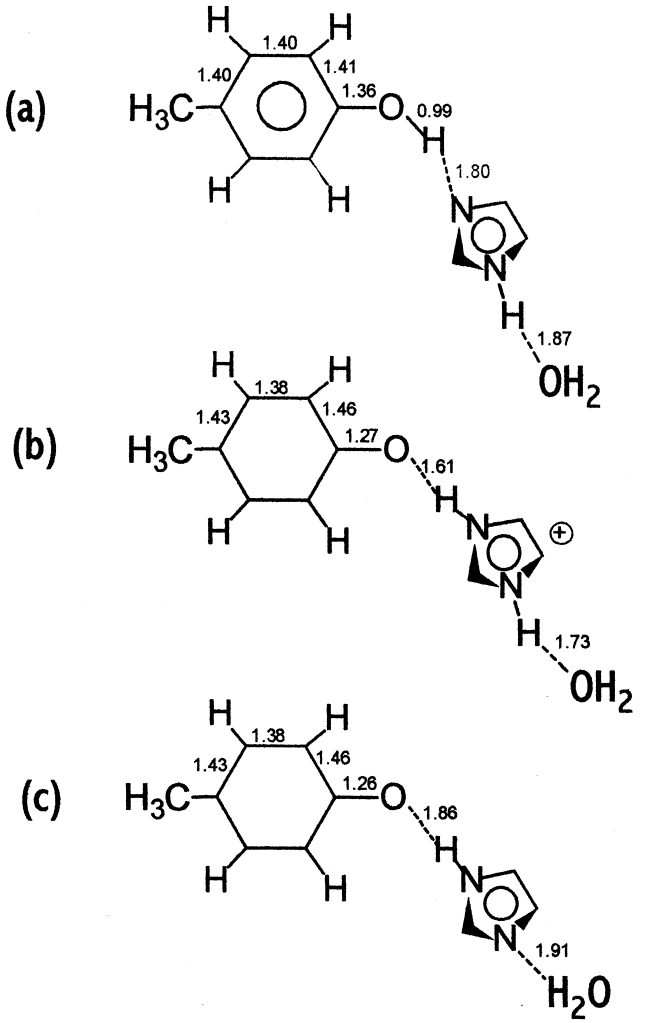

Fig. 2. Extended complexes of Fig. 1, with water, used to model additional hydrogen bonding interactions to the imidazole/imidazolium group; (a) MePH-IM-HB, (b) MeP-IMH-HB^{+}• and (c) MeP-IM-HB•. Selected optimised bond distances are given in Å.

Table 1
Comparison of calculated and experimental frequencies, cm^{-1}, for the reduced forms

System	Normal isotopes		$^{13}C(4)$		$^{13}C_6$		$^{2}H_4$	
	7a	δCOH	7a	δCOH	7a	δCOH	7a	δCOH
Theory								
MePH	1261 [98]	1173 [131]						
MePH-IM	1283 [91]	1247 [152]	1261 (−22)	1232 (−15)	1251 (−32)	1222 (−25)	1236 (−47)	-
MePH-IM-HB	1283 [91]	1250 [150]	1262 (−21)	1234 (−16)	1252 (−31)	1225 (−25)	1238 (−45)	
Experimental								
p-Cresol/CCl_4	1255	1175	ND	ND	ND	ND	ND	ND
p-Cresol/imidazole	1271	1251	ND	ND	ND	ND	1226 (−45)	ND
Y_D	1275	1250	ND	1226 (−24)	ND	1220 (−30)	1230 (−45)	ND
Y_Z	1279	1255	ND	1234 (−21)	ND	1230 (−25)	1233 (−46)	ND

Intensity (km/mol) and isotope shift values are given in brackets and parentheses respectively. Experimental values are as given in [12,13].
ND, not determined experimentally; $^{13}C(4)$ labelling at C4 atom position; $^{13}C_6$ labelling at all six phenol ring carbons; $^{2}H_4$ labelling at all four phenol ring hydrogens.

found previously for phenol–imidazole hydrogen bonded complexes [18]. A similar finding has been reported by Bloomberg et al. [19]. The geometry of the resultant positively charged radical complexes, MeP-IMH$^+$• and MeP-IMH-HB$^+$•, are given in Figs. 1c and 2b. The scaled harmonic frequency values calculated for the 7a CO stretching mode are given in Table 2 and compared with experimental determinations for Y_Z• and Y_Z•. The shifts in frequency for the various isotopomers are also given in Table 2. It is clear from this table that the MeP-IMH$^+$• and MeP-IMH-HB$^+$• models impressively reproduce the experimental values measured for the in vivo radicals. The fate of the phenol proton released on Y_Z and Y_D oxidation has been the subject of some debate in the literature [7,8]. It has been suggested that, rather than being localised as an imidazolium ion (Fig. 3a), the proton can be transferred to a larger, more distant, base acceptor pool (Fig. 3b), or at the limit a domino effect operates and the proton is transferred ultimately to the outside solution (Fig. 3c). The latter scenario would result in the situation represented by the MeP-IM• model of Fig. 1d where the tyrosyl residue is interacting with a neutral imidazole moiety. The calculated harmonic frequency data of Table 2 show that the MeP-IM• model does not exhibit good agreement with the experimental determinations for Y_D• and especially Y_Z•. Introduction of another hydrogen bond to the free imidazole nitrogen as modelled by MeP-IM-HB• leads to essentially unchanged values for the 7a mode (Table 2). Hydrogen bonding to the oxygen atom in phenoxyl radicals has been shown to lead to an increase in the 7a mode frequency value [20]. The upward shift in frequency, on hydrogen bond formation, for the 7a mode of phenoxyl type radicals[1] is directly proportional to the hydrogen bond strength. The weaker hydrogen bond donation in MeP-IM• results therefore in a lower perturbation of the 7a mode form. A reasonable interpretation of the above data is that Y_Z• and Y_D• correspond to the situation modelled by MeP-IMH$^+$• or MeP-IMH-HB$^+$•, or at least to a situation where the charge is located close to the tyrosyl free radical. The frequency value and the isotope shifts are in quite good agreement with experimental determinations. The phenol proton released on Y_Z oxidation is retained close to the tyrosyl radical retaining a strong hydrogen bond link between the D1-His190 and the Y_Z• radical and is readily available for back transfer on reduction of Y_Z• by the manganese complex. For Y_D• the lower 7a mode value compared with Y_Z• suggests a weaker hydrogen bonding interaction between D2-His189 and Y_D• than with Y_Z• and D1-

[1] A downshift for a pure CO stretching mode frequency value is expected on hydrogen bond formation. For phenoxyl free radicals we have previously shown [20] that ion formation or strong hydrogen bonding to the phenoxyl oxygen significantly changes the 7a mode form, leading to a greater degree of ring movement. This additional atom movement in the mode form is the most likely reason for the upshift in frequency value predicted.

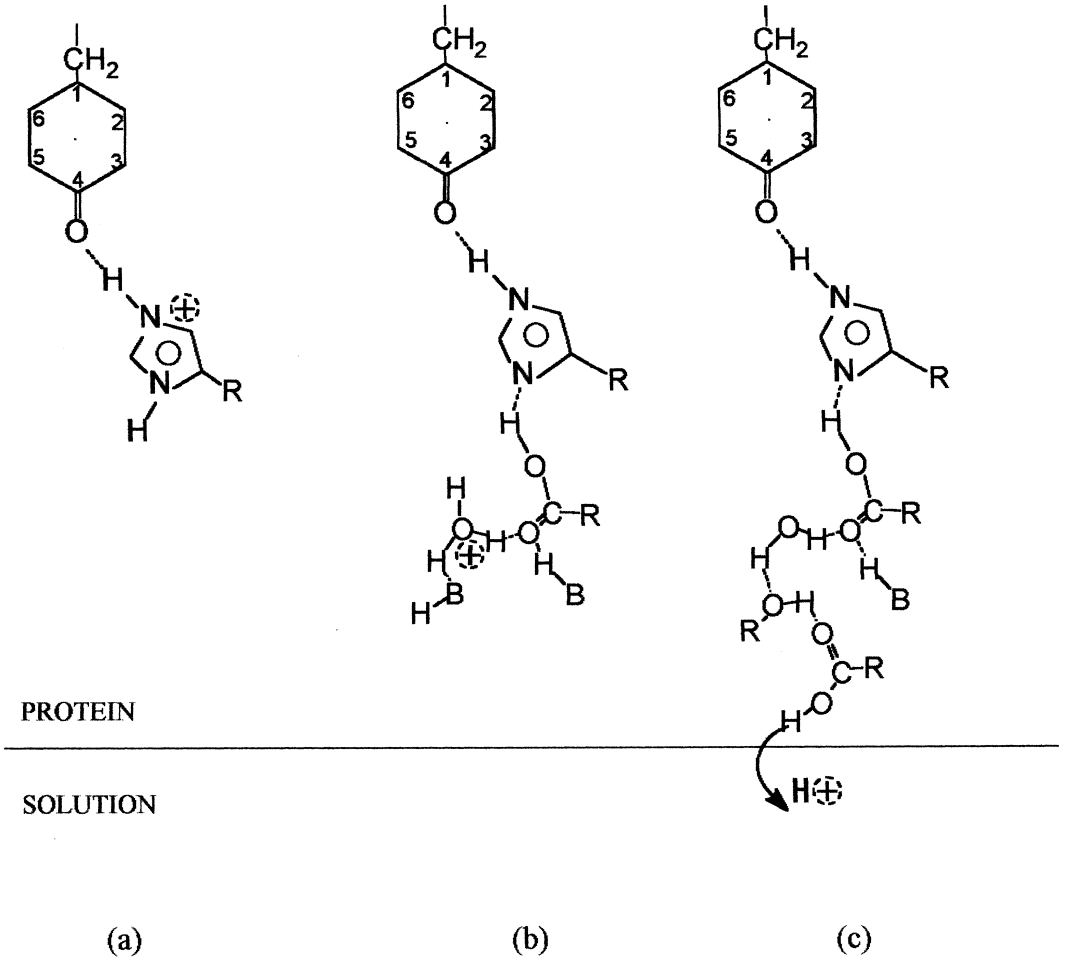

Fig. 3. Schematic view of proton localisation/delocalisation after Y_D or Y_Z oxidation. See text for details. Adapted from [2] (a).

Table 2
Comparison of experimental and calculated 7a frequency and isotope frequency shifts for the oxidised forms

System	ν_{7a}	$\Delta\nu_{7a}$ $^{13}C(4)$	$\Delta\nu_{7a}$ $^{2}H_4$	$\Delta\nu_{7a}$ $^{13}C_6$
Theory				
MeP-IMH^{+}•	1515	−27	−17	−41
MeP-IMH-HB^{+}•	1508	−31	−16	−39
MeP-IM•	1493	−29	−24	−40
MeP-IM-HB•	1492	−29	−24	−40
Experimental				
Y_Z•	1512	−27	−16	−36
Y_D•	1503	−26	−17	−35

Experimental values are as given in [12,13].
$^{13}C(4)$ labelling at C4 atom position; $^{13}C_6$ labelling at all six phenoxyl ring carbons; $^{2}H_4$ labelling at all four phenoxyl ring hydrogens.

His190. Indeed the data of Table 2 suggest that the difference in stretching frequency for the 7a mode of Y_D• and Y_Z• could be simply due to the presence or absence of a hydrogen bond to the imidazolium moiety. More generally it may imply that the proton charge released on oxidation of the tyrosine residue is more delocalised for Y_D• compared with Y_Z•. Such a situation would also explain the lower redox potential of Y_D• compared with Y_Z• and the greater stability/lifetime of Y_D• [21]

It is important to point out that the experimental FTIR data used here were recorded either for systems in which oxygen evolution was inhibited by use of the apoenzyme (Mn depleted) or on systems depleted of Ca. The data presented in [13] suggest, however, that the removal of the manganese complex has little effect on the D1-Tyr161–D1-His190 hydrogen bond as the FTIR data are identical for the in-

tact and apoenzyme. It is also of note that FTIR data obtained by Noguchi et al. [22] on the functional enzyme for Y_Z appear to be identical to the inhibited systems. This suggests that these inhibitory treatments do not disturb the hydrogen bond between D1-His190 and D1-Tyr161. The reported effects on Y_Z oxidation kinetics caused by such treatments [23,24] are unlikely to be due to a perturbation of this link.

As indicated in Section 1 it has been recently suggested by Barry and coworkers [14] that the assignments in [12,13] are incorrect and the infrared bands arise due to deleterious buffer conditions rather than from the PSII tyrosines. It should however be pointed out that the key data presented in [12,13] have been reproduced independently by Noguchi et al. [22]. It is also clear from the data presented in this report that the data presented in [12,13] are completely consistent with density functional calculations on models of hydrogen bonded tyrosine and tyrosyl radicals. On the other hand the tyrosyl 7a frequency value of 1478 cm^{-1} reported by Kim et al. [14] is about 20 cm^{-1} lower than any phenoxyl or tyrosyl 7a value reported in the literature either in vitro or in vivo. The isotope shifts reported for this band, -9 cm^{-1} for the $^2H_4$ isotopomer and -55 cm^{-1} for the $^{13}C_6$ isotopomer, also disagree with the calculated shifts presented in Table 2. We conclude therefore that the experimental FTIR data presented by Hienerwadel et al. [12] and Berthomieu et al. [13] are a true reflection of tyrosine oxidation for Y_D and Y_Z respectively.

References

[1] P. Reichard, A. Ehrenberg, Science 221 (1983) 514.

[2] C.W. Hoganson, G.T. Babcock, in: H. Sigel, A. Sigel (Eds.), Metal Ions in Biological Systems, Vol. 30, Marcel Decker, New York, 1994, pp. 77–107.

[3] W.J. Smith, T.E. Eling, R.J. Kulmacz, L.J. Marnett, A.L. Tsai, Biochemistry 36 (1997) 9356.

[4] A. Ivanchich, J.-M. Jouve, B. Sartor, J. Gaillard, Biochemistry 36 (1997) 9356.

[5] G.T. Babcock, M.K. El-Deeb, P.O. Sandusky, M.M. Whittaker, J. Am. Chem. Soc. 114 (1992) 3727.

[6] F. Macmillan, A. Kannt, J. Behr, T. Prisner, H. Michel, Biochemistry 38 (1999) 9179.

[7] G.T. Babcock, C. Tommos, Biochim. Biophys. Acta 1458 (2000) 199.

[8] R. Ahlbrink, M. Haumann, D. Cherepanov, O. Bogerhausen, A. Mulkidjanian, W. Junge, Biochemistry 37 (1998) 1131.

[9] L.P. Candeias, S. Turconi, J.H.A. Nugent, Biochim. Biophys. Acta 1363 (1998) 1.

[10] M. Haumann, W. Junge, Biochemistry 38 (1999) 1258.

[11] W. Mantele, Trends Biochem. Sci. 18 (1993) 197.

[12] R. Hienerwadel, A. Boussac, J. Breton, B.A. Diner, C. Berthomieu, Biochemistry 36 (1997) 15447.

[13] C. Berthomieu, R. Hienerwadel, A. Boussac, J. Breton, B.A. Diner, Biochemistry 37 (1998) 10547.

[14] S. Kim, J.S. Patslaff, T. Krick, Ayala, R.K. Sachs, B.A. Barry, J. Phys. Chem. B 104 (2000) 9720.

[15] Y. Qin, R.A. Wheeler, J. Chem. Phys. 102 (1995) 12995.

[16] Y. Qin, R.A. Wheeler, J. Am. Chem. Soc. 117 (1995) 6083.

[17] Y. Qin, R.A. Wheeler, J. Phys. Chem. 100 (1996) 10554.

[18] P.J. O'Malley, J. Am. Chem. Soc. 120 (1998) 11732.

[19] M.R.A. Bloomberg, P.E.M. Siegbahn, G.T. Babcock, J. Am. Chem. Soc. 120 (1998) 8812.

[20] P.J. O'Malley, Chem. Phys. Lett. 325 (2000) 69.

[21] B.A. Diner, X.-S. Tang, M. Zheng, G.C. Dismukes, D.A. Force, D.W. Randall, R.D. Britt, in: P. Mathis (Ed.), Photosynthesis: from Light to Biosphere, Vol. II, Kluwer Academic, Dordrecht, 1995, pp. 229–234.

[22] T. Noguchi, Y. Inoue, X.-S. Tang, Biochemistry 36 (1997) 14705.

[23] A.-M.A. Hays, I.R. Vassilev, J.H. Golbeck, R.J. Debus, Biochemistry 37 (1998) 11352.

[24] A.-M.A. Hays, I.R. Vassilev, J.H. Golbeck, R.J. Debus, Biochemistry 38 (1999) 11852.